Published in final edited form as:
J Comp Neurol. 2010 September 1; 518(17): 3409–3426. doi:10.1002/cne.22428.

Calcium-Binding Protein Immunoreactivity Characterizes the Auditory System of *Gekko gecko*

Kai Yan[1], **Ye-Zhong Tang**[2], and **Catherine E. Carr**[1,*]

[1]Department of Biology, University of Maryland, College Park, Maryland 20742

[2]Chengdu Institute of Biology, Chinese Academy of Sciences, 610041 Chengdu, People's Republic of China

Abstract

Geckos use vocalizations for intraspecific communication, but little is known about the organization of their central auditory system. We therefore used antibodies against the calcium-binding proteins calretinin (CR), parvalbumin (PV), and calbindin-D28k (CB) to characterize the gecko auditory system. We also examined expression of both glutamic acid decarboxlase (GAD) and synaptic vesicle protein (SV2). Western blots showed that these antibodies are specific to gecko brain. All three calcium-binding proteins were expressed in the auditory nerve, and CR immunoreactivity labeled the first-order nuclei and delineated the terminal fields associated with the ascending projections from the first-order auditory nuclei. PV expression characterized the superior olivary nuclei, whereas GAD immunoreactivity characterized many neurons in the nucleus of the lateral lemniscus and some neurons in the torus semicircularis. In the auditory midbrain, the distribution of CR, PV, and CB characterized divisions within the central nucleus of the torus semicircularis. All three calcium-binding proteins were expressed in nucleus medialis of the thalamus. These expression patterns are similar to those described for other vertebrates.

Keywords

cochlear nucleus; magnocellularis; laminaris; angularis; torus

Over 30 years have passed since Foster and Hall (1978) reported that the ascending auditory pathways of the iguana resemble both the mammalian and the avian auditory pathways, from the level of the first-order neurons in the VIIIth nerve to the telencephalon. They recognized a basic plan for the organization of the auditory system in terrestrial vertebrates but also pointed out that the auditory capacities of the lizards were largely unknown. We now know more about the peripheral (Manley, 1990; Wever, 1978) and central (for reviews see Carr, 1992; Grothe et al., 2005; ten Donkelaar et al., 1987) auditory systems of lizards, but still know little about central auditory processing. We have therefore used *Gekko gecko* for further analysis of the lizard central auditory system.

Geckos are auditory specialists that use vocalizations for intraspecific communication (Marcellini, 1977; Tang et al., 2001). Their ears differ from those of other reptiles such as archosaurs and turtles. Lepidosaur ears are highly directional, with middle ears connected through the mouth cavity (Christensen-Dalsgaard and Manley, 2008). This patent connection enhances the directionality of the ear by allowing sound access to both sides of

*CORRESPONDENCE TO: Catherine E. Carr, Department of Biology, University of Maryland, College Park, MD 20742. cecarr@umd.edu.

each tympanic membrane. The acoustically coupled ear creates directional responses from the tympanum (Christensen-Dalsgaard and Manley, 2005, 2008). Additionally, lizards have independently evolved micromechanical hair cell tuning, permitting emergence of sensitive high-frequency hearing in a specialized region of the papilla (Manley, 2002). Thus lizard auditory systems might reveal specializations for hearing high frequencies and sound localization.

We have begun our analysis of lizard auditory systems by using immunohistochemical techniques to delineate the auditory nuclei of *Gekko gecko* and to allow comparison with auditory pathways in other Reptilia (birds) and mammals. In archosaurs, like birds and crocodilians, the auditory nerve enters the brain and divides in two, with the ascending branch terminating in the nucleus angularis and the descending branch in the nucleus magnocellularis. The nucleus magnocellularis projects to the binaural nucleus laminaris, which in turn projects to the superior olive, to the lemniscal nuclei, and to the central nucleus of the auditory midbrain. The nucleus angularis projects to the superior olive, to the lemniscal nuclei, and to the central nucleus of the auditory midbrain. The parallel ascending projections of angularis and laminaris may or may not overlap with one another and probably do overlap in the primitive condition (for reviews see Carr, 1992; Carr and Code, 2000). The connections of the central auditory system are well known in mammals and follow a similar ascending trajectory (for reviews see Grothe et al., 2005; Rouiller, 1997). Mammalian ascending auditory pathways are characterized by monaural projections from the first-order nuclei to the superior olivary nuclei and the nuclei of the lateral lemniscus and by binaural projections from the olivary nuclei (Cant and Benson, 2003). These pathways converge in the auditory midbrain, or inferior colliculus.

In both birds and mammals, calcium-binding proteins have proved to be useful markers for specific functional auditory pathways. They label neurons in the central auditory system of mammals such as rat (Lohmann and Friauf, 1996; Pór et al., 2005), guinea pig (Caicedo et al., 1996), and human (Bazwinsky et al., 2003); in birds such as chicken (Parks et al., 1997) and barn owl (Kubke et al., 1999; Takahashi et al., 1987); and in lizards (Dávila et al., 2000), turtles (Belekhova et al., 2004), and amphibians (Morona and González, 2009). We therefore used antibodies against calretinin (CR), parvalbumin (PV), and calbindin-D28k (CB), along with antibodies against glutamic acid decarboxylase (GAD) and synaptic vesicle protein 2 (SV2), to describe the gecko ascending auditory pathways.

We also used antibodies against GAD to determine the distribution of GABAergic neurons and terminals in the auditory nuclei. GAD antibodies had previously been used to study the auditory system of barn owl and chick (Carr et al., 1989; Lachica et al., 1994; Müller, 1987; von Bartheld et al., 1989). SV2 is a component of all vertebrate synaptic vesicles and is therefore a useful marker of synapses (Bindra et al., 1993; Buckley and Kelly, 1985). Differential expression of calcium-binding proteins characterizes the structures of the gecko auditory system and reveals significant similarities to auditory structures in archosaurs, turtles, mammals, and amphibians.

MATERIALS AND METHODS

This study was based on data from 28 adult *Gekko gecko* of both sexes. All animal care and anesthesia procedures followed the procedures approved by the University of Maryland College Park Animal Care And Use Committee. Geckos were anesthetized in a mixture of isofluorane and room air in a small chamber, followed by i.p. injection of euthasol at a dose of 7 mg/kg. Once the geckos were deeply anesthetized (no response to toe pinch, depressed respiration), they were perfused transcardially with 0.9% saline, followed by 4% paraformaldehyde in 0.1 M phosphate buffer for 1 hour. The brains were postfixed in the

fixative overnight at 4°C and cryo-protected in 30% sucrose in 0.1 M phosphate buffer at 4°C. The brains were sectioned on a freezing microtome at 40 μm thickness, and all the sections were collected in order in phosphate buffer. Most brains were cut in the coronal plane, with three brains cut in the horizontal and two in the sagittal plane.

Immunohistochemical procedures used the avidin-biotin-peroxidase complex (Vector Laboratories) method in conjunction with horseradish peroxidase substrate reagent SG kits (Vector Laboratories, Burlingame, CA). Free-floating sections were preincubated for 1 hour in a blocking solution of 10% normal goat serum diluted in 0.1 M phosphate-buffered saline (pH 7.4) containing 0.3% Triton X-100. Subsequently, sections were incubated with antisera against 1) CR (7699/66; Swant, Belinzona, Switzerland) diluted in 1:5,000; 2) PV (PA-235; Sigma, St. Louis, MO) diluted 1:2,000; 3) CB (300; Swant) diluted in 1:3,000; 4) GAD (G5163; Sigma) diluted 1:1,000; 5) SV2 (Hybridoma Bank, University of Iowa) diluted in 1:1,000 for 2 days at 4°C (Table 1). After multiple washes, sections were incubated for 1 hour in biotinylated goat anti-rabbit (for GAD, CR) or goat anti-mouse (for PV, CB, SV2) secondary antisera, diluted 1:500. Sections were incubated in ABC, followed by a horseradish peroxidase reaction. Sections were then mounted, dried, dehydrated, and coverslipped. Some sections were additionally counter-stained with neutral red.

Cerebellar tissue was used to optimize staining patterns. It was incubated in the presence or absence of primary antibodies, and, in their absence, immunostaining of Purkinje cells and granule cells was eliminated. By contrast, the Purkinje cells heavily expressed CB and PV but not CR, whereas CR labeled stellate cells (Bastianelli, 2003). Serial dilution controls were used to optimize the working concentration of each antibody. Four serial dilutions of primary antibody ranged from 1:500 to 1:16,000, and sections were processed as described above, shared common reaction baths, and were incubated simultaneously. We measured the optical density of labeled neurons with respect to antibody dilution, and all antibody concentrations used were in the linear stages of the optical density vs. concentration plot. The dilution used for PV (1:2,000) was at the high end of the linear range because of light staining for PV in gecko (Fig. 1). To double-label CR and PV or CB, sections were incubated in two primary antisera simultaneously. After washing, sections were incubated in a mixture of two secondary antibodies, Alexa 594 donkey anti-rabbit and Alexa 488 donkey anti-mouse (Invitrogen, Carlsbad, CA) in the dark at a dilution of 1:500. The labeled sections were coverslipped with an antifade kit (Invitrogen), and images were obtained with a confocal microscope (Zeiss LSM 510). Digital images of selected sections were captured either on the confocal microscope or with a digital camera (DVC, Austin, TX) mounted on an Olympus BX-60 microscope. Image contrast adjustments and photomontages were performed in Adobe Photoshop 11 (Adobe Systems, Mountain View, CA).

Antibody characterization

Western blots were used to examine antibody specificity (Fig. 1). A gecko brain was removed after the animal had been deeply anesthetized as described above. Pre-chilled RIPA buffer containing a protease inhibitor mixture was added at a volume of 5 ml/g tissue, and the tissue was broken down by homogenizer and vortex for 60 seconds. The suspension was stored on ice for 45 minutes, followed by centrifugation at 14,000*g* for 10 minutes at 4°C. Cytosolic protein was collected from the supernatant, whose concentration was measured by Bradford protein assay (Bio-Rad, Hercules CA). Ten micrograms protein and 5 μl standard (161-0324; Bio-Rad) were loaded onto 12% SDS-PAGE gels. The protein was separated by SDS-PAGE and transferred to a PVDF membrane. The membrane, blocked with TBST containing 3% BSA for 1 hour at room temperature, was incubated in primary antisera diluted to 1:2,000 in 1% BSA in TBST overnight at 4°C. Afterward, it was probed with alkaline phosphataseconjugated goat anti-rabbit or goat anti-mouse (1:5,000; 31340 and 31320; Pierce, Rockford, IL) for 1 hour at room temperature. The blots were visualized by

exposing the membrane to ECF substrate (Amersham Bioscience, Piscataway, NJ) in the dark for 5–10 minutes and scanned on Storm (Molecular Dynamics, Sunnyvale, CA).

Blots with CR showed a major band at an estimated molecular weight of 29 kD, similar to the measurement in chick (Hack et al., 2000). CB, PV, and GAD blots also yielded single bands at estimated molecular weights of 28 kD (Ellis et al., 1991), 15 kD (Celio, 1990; Lohmann and Friauf, 1996) and 65–67 kD (Sloviter and Nilaver, 1987), respectively (Fig. 1). Western blot analysis of the anti-SV2 antibody had previously been tested against zebra finch brain tissue and produced a broad band over a range of protein sizes of 66–200 kD (Nealen, 2005). This may be due to the difficulty in electrophoretically resolving glycoproteins. Our Western blot of SV2 against gecko brain tissue showed multiple bands around 200 kD, within the range of results for zebra finch (Fig. 1).

RESULTS

The auditory nerve in gecko projects to two first-order nuclei, the nucleus magnocellularis (NM) and the nucleus angularis (NA; Figs. 2A, 3; Szpir et al., 1990). NM is divisible into two subregions, a caudal and medial NMM and a lateral rostral NML located caudal to NA (Figs. 2A, 3A,B; Szpir et al., 1990). We also recognize a nucleus laminaris (NL) ventral to NM. NA is the largest hindbrain auditory nucleus and contains a more heterogeneous grouping of cells than NM and NL. The superior olivary nuclei (SO) are located in the ventral hindbrain and consist of two separate nuclei, the SO proper and a ventral SO. The nuclei of the lateral lemniscus are made up of a dorsal nucleus with anterior and posterior divisions (LLD; Fig. 2E,F). These auditory nuclei project to the midbrain torus semicircularis (Foster and Hall, 1978).

Neurons in the auditory ganglion, first-order nuclei, and nucleus laminaris express multiple calcium-binding proteins

The posterior root of the VIIIth nerve receives fibers from the macula of the sacculus, the posterior ampullary crista, the macula neglecta, and the macula lagenae and papilla basilaris of the cochlear duct (Barbas-Henry and Lohman, 1988). The auditory fibers occupy the most dorsal position of the nerve root, which enters the brainstem slightly more caudally than the vestibular division of the posterior root (Barbas-Henry and Lohman, 1988; Miller, 1975). In the gecko, the auditory portion of the nerve contains two distinct bundles of fibers, one dorsal and caudal to the other (Fig. 2C). The dorsal-caudal fiber bundle bifurcates upon entering the brainstem. One branch runs caudally to the NMM and to the NML, whereas the other branch terminates more rostrally in the lateral division of the nucleus angularis (NAL). The second bundle is more ventral and rostral in the nerve and appears to project only to medial NA (NAM; Fig. 2A,C). Szpir et al. (1995) describe the projection to NAM in the alligator lizard as a sphere at the tip of the bundle of ascending, free-standing fibers; a similar pattern is observed in the gecko, in which immunoreactive auditory nerve fibers enter NA dorsally and branch to a semicircular array of NAM neurons. The auditory nerve expresses multiple calcium-binding proteins; CR-immunoreactive (CR-ir) fibers project to NM and NA via CR-ir auditory ganglion neurons. Comparisons of CR-ir and SV2-ir material reveal CR-ir synaptic terminals in NM and NA, including those of the auditory nerve (Figs. 2B–D, 3, 4). Similarly, PV- and CB-ir labeled most auditory nerve fibers (Fig. 4).

Postsynaptic neurons in NM and NA are densely CR-ir (Figs. 3–5). NM contains large CR-ir cell bodies termed *ovoid neurons* (Szpir et al., 1995). The caudal and medial NM (NMM) contained larger ovoid cells (mean diameter 12.3 ± 1.47 μm, mean area 108.9 ± 24.9 μm^2, n = 78) and the more rostral and lateral NML contains smaller ovoid cells (mean diameter 11.1 ± 1.5 μm, mean area 86.2 ± 21.6 μm^2, n = 78; two tailed *t*-test $P = 6.01 \times 10^{-8}$). The

eponymously named ovoid cells have cell bodies with aspect ratios of 0.85 ± 0.1 for NMM and 0.82 ± 0.1 for NML.

Below NM, ventrally located, bitufted CR-ir neurons form the second-order nucleus laminaris (NL; Figs. 3G,H, 4B,E). These neurons are a bit larger (mean area 119.8 ± 24.6 μm^2, n = 25) and more oval (mean aspect ratio = 0.73 ± 0.05, n = 25) than the overlying NML neurons. The dorsal CR-ir dendrites of NL extend into the overlying NM, whereas ventral dendrites extend below the cell body lamina. Laterally, NL merges with NML, with no clear border between the cell groups. Auditory nerve axons and terminals in NA and NM are also densely CB-ir and PV-ir (Figs. 3–5). Additionally, neurons in NM and NL cytoplasm are lightly CB-ir (Figs. 3D, 4).

Double-label immunofluorescence was used to determine whether calcium-binding proteins are localized within the same neurons. Most auditory nerve ganglion cell bodies, and their terminals in NM and NA, are immunoreactive for CR, CB, and PV (white, Fig. 4A,C,D,F). In double-labeled material, NM neurons and auditory nerve terminals are strongly CR-ir, auditory nerve terminals are also CB-ir, and CB is expressed at lower levels in the cytoplasm of NM neurons beneath the membrane (Figs. 3, 4). In double-labeled material, NL neurons and neuropil are strongly CR-ir, lightly CB-ir, and not PV-ir (Fig. 4B,E). In NA, the nerve terminals coexpress CR, PV, and CB, and a small population of NA neurons coexpresses CR and CB (Figs. 4C,F, 5). NA neurons were similar in size to NM (mean diameter 12.07 ± 1.92 μm, mean area 105.6 ± 33.2 μm^2, n = 70). Many of the ascending axons from the first-order nuclei are CR-ir (see Figs. 2, 6, 7, 9).

GAD-ir presynaptic terminals surrounded unlabeled somata in NM (Fig. 3F). GAD-ir terminals differ from auditory nerve terminals in their distribution and small size and are abundant in NM and NL and sparser in NA. There is a small population of GAD-ir neurons in NA, NL, and NM. Somatic GAD-ir varies in intensity from light to medium, and GAD-ir neurons are not otherwise distinguishable from unlabeled NM or NA neurons; NM GAD-ir neurons have mean areas of 90.7 μm^2 (±26.78, n = 19), and NA GAD-ir neurons have mean areas of 91 μm^2 (±26.8, n = 35; Fig. 5E).

Superior olivary nuclei receive CR-ir terminals

There are two superior olivary nuclei, one dorsal and one ventral (Figs. 2E, 6). Both form rostrocaudally directed cell columns, with the ventral nucleus originating at just caudal to the lemniscal nuclei and extending to the level of the first-order nuclei. The ventral olivary nucleus (SOv) was named the *nucleus of the trapezoid body by* Foster and Hall (1978), but we will refer to it as the *ventral olivary nucleus* in order not to imply homology with the nuclei of the same name in mammals. The nucleus of the superior olive proper (SO) is a round nucleus in the rostral pons, ventral to NL (Figs. 2F, 3, 6). Distinct calcium-binding protein expression patterns delineate both the nucleus of the superior olive and the ventral nucleus. Both contain dense CR-ir fibers with large boutons surrounding unlabeled neurons (Fig. 6C,F). In both nuclei, bouton size is not normally distributed. Both large and very large CR-ir boutons are distributed throughout the neuropil. In the superior olive, the large boutons have areas of 4 μm^2 (±1.2, n = 92), whereas about 24% of boutons are very large, with areas larger than 7 μm^2 (mean 11.1 ± 2.75 μm^2,n = 19). The same pattern is found in the ventral nucleus, with large bouton areas of 4.2 μm^2 (±1.5, n = 22), whereas about 24% of boutons are very large, with areas larger than 7 μm^2 (mean 11 ± 3.1 μm^2,n = 17). In the ventral nucleus, many large boutons are perisomatic.

The CR-ir fibers in the olivary nuclei appear to originate from the first-order nuclei and/or NL and project to both the ipsilateral and the contralateral olivary nuclei (arrows in Fig. 7B). No postsynaptic elements in the olivary nuclei are CR-ir. The SO and Sov contain CB-ir cell

bodies and terminals, with CB-ir cell bodies often concentrated in the dorsal portion of SO (see Fig. 8B,C). Both cell bodies and neuropil in the SO and SOv are PV-ir (Fig. 6A), and dense GAD-ir terminals are found in both olivary nuclei, both perisomatically and distributed throughout the neuropil (Fig. 8D, SO). About one-third of the SO neurons are GAD-ir. Fewer GAD-ir neurons are observed in SOv.

The nucleus of the lateral lemniscus is predominantly GABAergic

In the gecko, the lemniscal nuclei are located in the lateral and rostral hindbrain, rostral to the ventral olivary nuclei (Foster and Hall, 1978). Labeled CR-ir axons ascend in the lateral lemniscus and delineate the tract connecting the SO, SOv, and lemniscal nuclei. Along their course, some of these fibers give off branches that terminate in the dorsal nucleus of the lateral lemniscus (LLD; Fig. 7). There appears to be no ventral nucleus of the lateral lemnsicus (see Discussion), and LLD is divided into anterior (LLDa) and posterior (LLDp) divisions, consistent with the avian nomenclature of Wild et al. (2009) and Wild (1987). LLDa and -p overlap throughout most of their extent, with the LLDp being both ventral and caudal to LLDa (Fig. 7). LLDp is larger than LLDa and is characterized by a preponderance of GAD-ir cell bodies and large, often perisomatic GAD-ir terminals. LLDa contains fewer GAD-ir cell bodies and dense, fine GAD-ir terminals (Fig. 7C,F).

Both LLD subdivisions contain CR-ir fibers and terminals, assumed to originate from the first-order nuclei, and no CR-ir somata. The CR-ir boutons are large (average diameter = 4.0 ± 2.2 μm, n = 95) and are distributed throughout the neuropil of LLD (Fig. 7D). In addition to the large CR-ir terminals, fine CB-ir, PV-ir, and GAD-ir terminals are distributed throughout the nuclei of LLD. GAD-ir, CB-ir, and PV-ir somata and neuropil characterize LLD (Fig. 7A–C). Although double-labeling experiments with these antibodies were not performed, GAD-ir neurons (mean 63.9 ± 24.7 μm^2,n = 13) are similar in area to PV-ir neurons (mean 63.7 ± 14.7 μm^2,n = 14; Fig. 7A,C).

The two LLD divisions differ in their proportion of GAD-ir neurons. LLDa contains evenly distributed GAD-ir terminals and few GAD-ir cell bodies; LLDp has many GAD-ir somata and larger GAD-ir terminals (Fig. 7C). The GAD-ir terminals encircle the LLDp cells and are also distributed throughout the neuropil. The GABAergic neurons of LLD are round (form factor mean = 0.91) and not otherwise cytologically distinct from the other cells in the nucleus. In GAD-ir material, LLDp contains both intensely immunoreactive and lightly immunoreactive cells. Insofar as all cells receive intensely immunoreactive perisomatic terminals, these differences in immunoreactivity did not appear to be due to insufficient penetration of the antibody. Varicose fibers and dendrites of these neurons form a network of GAD-ir elements in the nucleus. A third group of unstained cells receives perisomatic GAD-ir terminals.

Auditory midbrain and thalamus

The torus semicircularis is the homolog of the inferior colliculus in birds and mammals and is located caudal to and beneath the optic tectum. In lizards, the torus is divided into an auditory central nucleus, surrounded by intercollicular and preisthmic superficial areas (Browner and Rubinson, 1977; Díaz et al., 2000; Kennedy and Browner, 1981; Puelles et al., 1995; Smeets et al., 2006; ten Donkelaar et al., 1987). In this study, we will focus only on the central nucleus (TSc). The TSc is largest caudomedially, where it replaces the tectum at the dorsal midline. The caudal portion bulges outward, behind the caudal pole of the tectum, and is fused at the midline (Fig. 8; Kennedy and Browner, 1981). The TSc then extends lateroventrally under the tectum, where it is divided into left and right by the medial portions of the tectum and commissure of optic tectum.

The central nucleus is differentiated from the surrounding periventricular regions by distinct patterns of calcium-binding protein immunoreactivity. Within the central nucleus, several divisions have emerged. The entire central nucleus is marked by CB-ir cells and neuropil (Figs. 8–10). For the central nucleus, we define three subdivisions. The first is a lateral subdivision with large CR-ir fibers and terminals (average diameter = 4.5 ± 3.4 μm, n = 78), assumed to originate from the first-order nuclei (Figs. 9A,D, 10A). The second central nucleus subdivision is delineated by intensely immunoreactive PV-ir neuropil in the ventral portion of the central nucleus (Figs. 8A, 10B, cf. Belekhova et al., 2004). The CR-ir and PV-ir subdivisions of the central nucleus overlap to a small degree (Fig. 10). In the caudal TSc, PV and CR are colocalized in some terminals. The third dorsomedial subdivision is characterized by CB-ir cells and neuropil and sparse CR-ir cell bodies with long CR-ir bipolar dendrites (Figs. 9C, 10).

Nucleus medialis is the auditory target in dorsal thalamus and is adjacent to the third ventricle. In both gecko (this study) and the lacertid lizard *P. algirus*, the nucleus medialis has a strongly CB-ir neuropil, with CB-ir neurons and fibers (Dávila et al., 2000). CB-ir neurons and fibers are both observed in the nucleus medialis (Fig. 11C). Some neurons in nucleus medialis are also PV-ir (Fig. 11D). The DVR, the target of nucleus medialis and the auditory region of the forebrain, was not evaluated in this study (Bruce and Butler, 1984).

DISCUSSION

Differential expression of calcium-binding proteins characterizes the structures of the gecko auditory system and reveals significant similarities to auditory structures in other vertebrates. The auditory nerve expresses high levels of these proteins, as do the neurons of the first-order nuclei, with distinct CR-positive terminal fields delineating their projection to olivary, lemniscal, and midbrain targets. The lemniscal nuclei are notable for the expression of markers for GABAergic neurotransmission, whereas examination of the midbrain torus revealed three distinct subdivisions in the central nucleus, a lateral first-order recipient zone marked by CR-positive terminals, a ventral core delineated by PV-positive neurons and terminals, and a large dorsomedial area. This study and the work of Robles-Moreno (1995) provide the first demonstrations of subdivisions within the central nucleus of the torus in a lizard.

Calcium-binding proteins in the auditory system

Calcium-binding proteins have proved to be useful markers in the gecko auditory system (Table 2). They are highly conserved and are abundant in the central auditory system (Celio and Heizmann, 1981). Calcium-binding proteins and cytochrome oxidase delineate the auditory system of terrestrial terrapins (*Testudo horsfieldi*) and pond tortoises (*Emys orbicularis*) in a pattern very similar to that observed in the gecko (Belekhova et al., 2004, 2008). Calcium-binding protein expression has also been described for auditory thalamic centers in the diencephalon of a lacertid lizard, *Psammodromus* algirus (Dávila et al., 2000).

Although the functional roles of calcium-binding proteins are unknown, CR is particularly abundant in auditory neurons with precisely timed discharges (Rogers, 1987; Schneggenburger and Neher, 2005). Both gecko and turtle auditory nerve and terminals express all three calcium-binding proteins (this study; Belekhova et al., 2008). Both turtle and gecko NM and NA neurons express both CR and CB, although the two are differently distributed within the cell body in gecko. Similarly, both avian NM (Hack et al., 2000) and mammalian globular bushy cells are characterized by high levels of CR, whereas globular bushy cells express CR and PV in their cytoplasm, and octopus cells express CR and CB (Bazwinsky et al., 2008; Pór et al., 2005). These abundant and often complementary calcium-binding protein distributions suggest a requirement for calcium regulation in these

auditory brainstem neurons, all of which are characterized by high rates of activity, phase-locked responses to auditory stimuli and calcium-permeable AMPA receptors (Christensen-Dalsgaard et al., 2007; Eatock et al., 1981; Otis et al., 1995; Raman and Trussell, 1995; Trussell, 1999, 2008). Colocalization of calcium-binding proteins and Ca-permeable glutamate receptors also characterizes other sensory systems, including the goldfish vagal lobe (Huesa et al., 2008; Ikenaga et al., 2006).

The ascending auditory projections from gecko first-order nuclei are characterized by high levels of CR-ir in their terminal fields in the olivary and lemniscal nuclei and in the torus, and our preliminary data suggest that CR-ir delineates these projections (Tang, unpublished). In birds, similar high levels of CR-ir characterize the ascending projection from the nucleus laminaris to the olivary nuclei, the anterior part of the dorsal nucleus of the lateral lemniscus, and the projection to the central nucleus of the inferior colliculus in the barn owl (Kubke and Carr, 2006; Kubke et al., 1999; Takahashi et al., 1987). In the gecko, it appears that most, if not all, ascending axons from the first-order nuclei and NL express CR, whereas, in the barn owl and chicken, the ascending NL axons are CR-ir, and those from NA are not (Takahashi et al., 1987).

Organization of the first-order nuclei

Lizard ears are highly directional, with middle ears connected through the mouth cavity (Christensen-Dalsgaard and Manley, 2005, 2008). The inner ears are also highly specialized, with sensitive high-frequency hearing in a specialized region of the papilla (Manley, 2002). Geckos have additional specializations of their auditory periphery; unlike other amniotes studied so far, the frequency map of the papilla is reversed, with the low frequencies at the base and the high frequencies at the apex (Manley et al., 1999). The high-frequency region of the papilla is split into two parallel hair cell areas, only one of which is innervated (Chiappe et al., 2007; Köppl and Authier, 1995).

These lepidosaur and geckkonid adaptations exert a noticeable effect on the first-order auditory nuclei. The high-frequency region of the papilla appears to have a separate projection to the brain, specifically to a large medial NA, as shown in the alligator lizard (Szpir et al., 1990). The reversed tonotopic gradient in the ear may or may not lead to a reversed tonotopic gradient in brain; this awaits a study to trace the projections of the auditory fibers into the first-order nuclei. Our data suggest that tonotopy may be reversed in NM, insofar as caudal NMM neurons are larger than NML neurons in geckos but not in alligator lizards (Szpir et al., 1990). Otherwise, we hypothesize that geckos have patterns of auditory nerve fiber projections similar to the pattern of alligator lizards, in which the auditory nerve fibers that contact low-frequency hair cells project to three of the four divisions of the first-order nuclei, NMM, NML, and NAL, whereas the auditory nerve fibers that innervate high-frequency hair cells project only to the NAM (Szpir et al., 1990). This hypothesis is supported by observations from our immunohistochemical material, in which a dorsal-caudal bundle of auditory nerve fibers enters the brain and bifurcates to project caudally to the NM and rostrally to lateral NA in geckos (see Fig. 2). A second more ventral and rostral fiber bundle forms a single branch that projects rostrally to medial NA. These findings are consistent with results from the alligator lizard (Szpir et al., 1990) and confirm Spzir et al.'s finding that two populations of auditory nerve fibers project to nonoverlapping first-order targets. Note that direct electrophysiological and anatomical evidence for the separation of the two nerve populations is presently lacking in gecko.

The first-order nuclei of the lizard have been described as showing a great deal of interspecific variation (for reviews see Carr and Code, 2000; Manley, 1981). In many lizards, four nuclear populations that receive primary auditory inputs have been recognized: a medial and lateral nucleus magnocellularis and a medial and lateral angularis (Miller,

1975). Alligator lizards have a distinct NMM, NML, NAM, and NAL (Szpir et al., 1995). Their NMM consists of a homogeneous population of neurons called *lesser ovoid* cells, whereas NML consists of "greater ovoid" and "small" cells. We observed similar large oval neurons in gecko NM but, unlike Szpir et al. (1995), found that the neurons of caudal NM (NMM) are larger than the neurons of the NML (see above). The alligator lizard NAL consists of smaller "spindle" cells, and NAM contains a population of large neurons called *duck-head* and *multipolar* cells and a population of smaller neurons called *bulb* and *agranular* cells (Szpir et al., 1995). We have not classified the NA neurons in gecko, but their size range is similar, although they are smaller.

In geckos, the ovoid cells in NMM are surrounded by perisomatic auditory nerve endings labeled with CR, PV, and SV2. Inasmuch as these terminals are perisomatic, they resemble the endbulb synapses in the avian NM and the mammalian AVCN, and the similarities suggest that they represent a homologous population corresponding to the NM of birds and turtles (Belekhova et al., 2008; Carr and Code, 2000; Grothe et al., 2005). Szpir et al. (1990) labeled individual axons and noted larger axosomatic terminals in NMM than in the other first-order nuclei.

Only some lizards have been reported to posses a distinct NL (ten Donkelaar et al., 1987). The conflicting reports in the literature may emerge from variation in the development of NM and NL. We recognize NMM, NML, NAM, NAL, and NL in *Gekko gecko*, although an NL was not previously observed in this species (Miller, 1975). NL is recognized on the basis of location below NM, bitufted neuronal architecture, chemical neuroanatomy, and similarity to NL in *Varanus exanthematicus* (Barbas-Henry and Lohman, 1988; ten Donkelaar et al., 1987) and *Iguana iguana* (Foster and Hall, 1978). In geckos, NL is a curved structure below NM, composed of two strands of CR-ir bipolar or spindle-shaped neurons with dorsoventrally directed dendrites, and merging laterally into NM. Gecko NL receives a projection from the contralateral acoustic tubercle (Tang et al., unpublished observations). Future tract tracing studies are needed to determine the projection cells of the acoustic tubercle; projection neurons that receive input from the contralateral NM may reasonably be identified as belonging to NL even if not cytologically distinct from the overlying NM. Alternatively, both NM and NL may provide ascending projections to the torus, and the separation in which only NL projects to the torus may be an archosaur adaptation.

Prior controversy over the presence or absence of NL may hinge on correct identification of NL rather than on a true absence or loss (Miller, 1975). For example, iguanas, like geckos, were also reported not to possess an NL, although Foster and Hall (1978) observed that NML did not appear to receive primary VIIIth nerve afferents and gave rise to projections to the midbrain. Similarly, NL is evident in geckos, consisting of a distinct population of bitufted CR-ir neurons below NM. Thus, although Miller (1975) writes that "I have never been able to define an unequivocal NL in lizards," the advent of modern tract tracing and immunohistochemical techniques may serve to unmask NL. In line with the hypothesis that NL characterizes all reptiles, snakes possess both cochlear nuclei and a nucleus laminaris (Miller, 1980). Their nucleus angularis is small, whereas nucleus magnocellularis has both medial and lateral divisions. The nucleus laminaris is well developed, and Miller states that the nucleus laminaris in a boid snake was better developed than that in any lizard examined (Erulkar, 1974; Miller, 1980). These findings are consistent with the new position of snakes, now nested with the anguimorph and iguanid lizards to form the Toxicofera (Vidal and Hedges, 2009). Finally, NL is well defined in turtles (Belekhova et al., 2008; Miller and Kasahara, 1979). Although more physiological and developmental data are needed (Grothe et al., 2005), the expression of CR, the bitufted neurons, the projection from the contralateral

acoustic tubercle, and the efferent projections to the torus are consistent with the hypothesis that lepidosaur and archosaur NL are homologous.

There are more GABAergic cells and terminals in the first-order nuclei than have been observed in birds (Carr et al., 1989; Lachica et al., 1994; Müller, 1987; von Bartheld et al., 1989). The GABAergic neurons and terminals in NA, NM, and NL are of unknown origin and function, but their presence may indicate an increased role of inhibition in shaping responses in an acoustically coupled ear (Christensen-Dalsgaard and Carr, 2008). Additionally, these GABAergic inputs may play a part in the transformation or sharpening of auditory nerve responses, as has been suggested for the avian first-order nuclei and the mammalian cochlear nuclei (Burger and Rubel, 2007; Caspary et al., 1979; Pollak et al., 2002). Without a suitable marker for glycine in gecko, we are unable to determine whether a glycinergic component is also present.

Organization of olivary and lemniscal nuclei

Identification of the superior olivary nuclei in reptiles has been complex (Belekhova et al., 2008). Unlike the case for birds, two olivary nuclei have been described for geckos and other reptiles. These are the dorsal superior olive and a smaller ventral superior olive (Ariens-Kappers et al., 1936; Foster and Hall, 1978; ten Donkelaar, 1998; ten Donkelaar et al., 1987). Belekhova has termed these nuclei the *supraolivary complex*. The ventral superior olive had previously been called the *nucleus of the trapezoid body* in iguana because it occupied a position similar to that of the trapezoid body of mammals (Foster and Hall, 1978). We will not use this terminology here, in order not to support or reject homology with mammals and to conform to Belekhova's terminology. Both superior olive and ventral superior olive appear to receive projections from the first-order nuclei and project to the torus in those lizards examined (Ariens-Kappers et al., 1936; Foster and Hall, 1978; ten Donkelaar, 1998; ten Donkelaar et al., 1987). A similar organization has been found in the terrapin *Testudo horsfieldi* and the tortoise *Emys orbicularis*. In these turtles, both olivary nuclei appear to receive input from the first-order nuclei, and the superior olive is connected by a clear fiber tract to the ventral superior olive, similar to that shown in our Figure 7B (Belekhova et al., 1985, 2008; Kunzle, 1986; Miller, 1980; ten Donkelaar, 1998). Patterns of calcium-binding protein expression in gecko olivary nuclei are similar to those observed in turtles, in which antibodies against PV and CB labeled both superior olive and ventral superior olive and in which both olivary nuclei are connected with a dense, intensively CR-ir bundle (Belekhova et al., 2008). These expression patterns are also similar to those observed in *Xenopus*, in which a densely labeled CB-ir bundle projected to the CR-ir superior olivary nuclei (Morona and González, 2009), and to those in mammals, in which CR-ir labels the fibers extending into the superior olivary complex and the nuclei of the lateral lemniscus (Lohmann and Friauf, 1996).

We have described a single lemniscal nucleus in gecko, consistent with results from *Iguana iguana* (Foster and Hall, 1978) and the pond turtle (Belekhova et al., 1985, 2008). Three nuclei are recognized in birds, dorsal, intermediate, and ventral (Arends and Zeigler, 1986; Wild et al., 2001, 2009). In birds, the ventral nucleus projects back to the first-order nuclei (Wild et al., 2009), the intermediate nucleus projects to thalamus (Wild et al., 2008; Wild, 1987), and the dorsal nucleus is largely GABAergic (Carr et al., 1989) and projects to the inferior colliculus (Fujita and Konishi, 1991). In birds, the dorsal nucleus is also reciprocally connected with its contralateral homologue via the commissure of Probst (Takahashi et al., 1995; Takahashi and Keller, 1992). For gecko, we identify a dorsal nucleus, also predominantly GABAergic, although tract-tracing studies are required to determine whether it projects to the torus and to its contralateral homologue. We are unable to determine whether an intermediate nucleus is present and hypothesize that the avian ventral nucleus of the lateral lemniscus is homologous to the ventral nucleus of the superior olive in lizards and

turtles. Embryological and tract tracing studies could be used to test this hypothesis. Currently, the most compelling reasons to homologize the avian ventral nucleus of the lateral lemniscus and lizard SOv are their immunohisto-chemical profile and topological position. In geckos, the dorsal nucleus of the lateral lemniscus occupies a similar location rostral to, and almost continuous with, the ventral superior olive (Belekhova et al., 2008; Takahashi and Konishi, 1988a). Developmental analyses of the hindbrain nuclei in chicken and quail embryos show that the avian superior olive is derived from rhombomeres 4 and 5, whereas the dorsal and ventral nuclei of the lateral lemniscus originate from rhombomeres 1–3 (Marin and Puelles, 1995). Embryological studies of the rhombomeric origins of individual auditory nuclei in lacertids and turtles may help to determine whether the avian ventral nucleus of the lateral lemniscus is more appropriately grouped with the olivary complex.

Organization of auditory midbrain

The torus semicircularis is the homolog of the inferior colliculus in birds and mammals and is located caudal to and beneath the optic tectum. In lizards, the torus was previously divided into a central nucleus, surrounded by laminar and superficial nuclei (Browner and Rubinson, 1977; Díaz et al., 2000; Kennedy and Browner, 1981; Smeets et al., 2006; ten Donkelaar et al., 1987). Only portions of the laminar nucleus correspond to the avian intercollicular nucleus, however, and Diaz et al. (2000) have proposed that use of this term be discontinued, because the area incorporates cytoarchitectonically distinct regions. In this study, we follow the subdivisions and some of the nomenclature introduced by Puelles et al. (1994) and Robles-Moreno (1995). We focus only on the auditory central nucleus of the torus or toral nucleus, separate from the surrounding areas, which are sometimes referred to as the *shell* (Zeng et al., 2007; Browner and Baruch, 1984; Browner and Rubinson, 1977). The central nucleus is the recipient of the lateral lemniscal fibers (Foster and Hall, 1978) and projects to the auditory nucleus of the thalamus (Foster and Hall, 1978; Kennedy and Browner, 1981; Pritz, 1974; ten Donkelaar et al., 1987). The reported auditory responses in previous studies were probably recorded in the TSc in *Gekko gecko* (Kennedy, 1974; Kennedy and Browner, 1981; Manley, 1981).

Immunoreactivity for CR, PV, and CB display distinct distribution patterns in the TSc. These distribution patterns suggest the presence of subdivisions within the central nucleus and different recipient zones for first-order, olivary, and lemniscal input. The existence of toral subdivisions confirms the hodological and immunohistochemical observations of Robles-Moreno (1995). Tract tracing combined with electrophysiological experiments are needed to determine whether the gecko TSc, like the torus and inferior colliculus in other vertebrates, has divisions based on different afferent inputs (for reviews see Covey and Carr, 2005; Schreiner and Winer, 2005). The restricted lateral distribution of CR-ir immunoreactive terminals in the TSc suggests that this is the recipient zone for input from NA and NL. We hypothesize that these CR-ir terminals originate from the CR-ir first-order nuclei and NL, because a CR-ir immunoreactive tract originates from NA and NL (Figs. 2, 7) and because the terminals in TSc are similar in size and shape those in SO and LLD. A second, ventral TSc division is PV-ir and may be the recipient zone for inputs from the LLD and the olivary nuclei, insofar as these nuclei contain many PV-ir neurons. These ideas must be tested by both physiological and tract tracing studies.

Turtles and anuran amphibians also display distinct distribution patterns in the torus, with a mostly complementary pattern of CR and CB in *Xenopus* (Morona and González, 2009) and a mostly complementary pattern of CR and PV in turtles (Belekhova et al., 2004). PV-ir predominates in a restricted core region of the central nucleus, with CR and CB-ir in the surrounding peripheral areas of the central nucleus. These complementary patterns of expression in amphibians and reptiles are similar to the patterns of CR and

acetylcholinesterase expression observed in the core and shell regions of the central nucleus of the barn owl inferior colliculus (Adolphs, 1993; Takahashi et al., 1987).

Separate, nonoverlapping projections from first-order, olivary, and lemniscal nuclei are somewhat incompatible with the tonotopy observed in the central nucleus of the auditory midbrain of mammals, archosaurs, and amphibians. In these vertebrates, the inferior colliculus is characterized by first-order projections throughout the central nucleus and by a dorsoventral low- to high-frequency tonotopy, although the pattern and frequency range differ (for reviews see Covey and Carr, 2005; Grothe et al., 2005). For the lizards, Browner and Rubinson (1977) reported that *Tupinambis nigropunctatus* exhibited tonotopic organization of the central nucleus of the auditory midbrain. Hartline and Campbell (1969) were able to record auditory responses in the midbrain of snakes, although the precise location of their recordings is not clear. If the gecko TSc is subdivided on the basis of afferent inputs, with projections from the first-order nuclei and NL being lateral and olivary and lemniscal projections ventral, then it is possible that separate tonotopically organized regions will be observed in the ventrolateral segment of the TSc or that tonotopic laminae abut, much as is the case in the barn owl inferior colliculus, in which input from NL to the central nucleus core abuts input of a similar best frequency from the lemniscal nuclei and the nucleus angularis into the central nucleus shell (Takahashi and Konishi, 1988a,b; Wagner et al., 2002).

Acknowledgments

We gratefully acknowledge Jakob Christensen-Dalsgaard's assistance with gecko surgery and anesthesia and L. Puelles and L. Bruce for help in identification of anatomical structures.

Grant sponsor: National Institutes of Health; Grant number: DC00436 (to C.E.C.); Grant number: P30 DC0466 (to the University of Maryland Center for the Evolutionary Biology of Hearing); Grant sponsor: Chinese Academy of Sciences Bairenjihua; Grant number: KSCX2-YW-R-077 (to Y.-Z.T.).

LITERATURE CITED

Adolphs R. Acetylcholinesterase staining differentiates functionally distinct auditory pathways in the barn owl. J Comp Neurol. 1993; 329:365–377. [PubMed: 7681456]

Arends J, Zeigler HP. Anatomical identification of an auditory pathway from a nucleus of the lateral lemniscal system to the frontal telencephalon (nucleus basalis) of the pigeon. Brain Res. 1986; 398:375–381. [PubMed: 3801910]

Ariens-Kappers, C.; Huber, G.; Crosby, E. The comparative anatomy of the nervous system of vertebrates, including man. Macmillan; New York: 1936.

Barbas-Henry HA, Lohman AHM. Primary projections and efferent cells of the VIIIth cranial nerve in the monitor lizard, Varanus exanthematicus. Brain Res. 1988; 398:375–381.

Bastianelli E. Distribution of calcium-binding proteins in the cerebellum. Cerebellum. 2003; 2:242–262. [PubMed: 14964684]

Bazwinsky I, Hilbig H, Bidmon HJ, Rubsamen R. Characterization of the human superior olivary complex by calcium binding proteins and neurofilament H (SMI-32). J Comp Neurol. 2003; 456:292–303. [PubMed: 12528193]

Bazwinsky I, Hartig W, Rubsamen R. Characterization of cochlear nucleus principal cells of Meriones unguiculatus and Monodelphis domestica by use of calcium-binding protein immunolabeling. J Chem Neuroanat. 2008; 35:158–174. [PubMed: 18065198]

Belekhova MG, Zharskaja VD, Khachunys AS, Gaidaenko GV, Tumanova NL. Connections of the mesencephalic, thalamic and telencephalic auditory centers in turtles. Some structural bases for audiosomatic interrelations. J Hirnforsch. 1985; 26:127–152. [PubMed: 2410486]

Belekhova MG, Kenigfest NB, Karamian OA, Vesselkin NP. Distribution of calcium-binding proteins in the central and peripheral regions of the turtle mesencephalic center torus semicircularis. Dokl Biol Sci. 2004; 399:451–454. [PubMed: 15717605]

Belekhova M, Chudinova T, Kenigfest N, Krasnoshchekova E. Distribution of metabolic activity (cytochrome oxidase) and immunoreactivity to calcium-binding proteins in the turtle brainstem auditory nuclei. J Evol Biochem Physiol. 2008; 44:354–364.

Bindra PS, Knowles R, Buckley KM. Conservation of the amino acid sequence of SV2, a transmembrane transporter in synaptic vesicles and endocrine cells. Gene. 1993; 137:299–302. [PubMed: 8299963]

Browner R, Baruch A. The cytoarchitecture of the torus semicircularis in the golden skink, Mabuya multifasciata. J Morphol. 1984; 180:223–242.

Browner R, Rubinson K. The cytoarchitecture of the torus semicircularis in the tegu lizard, Tupinambis nigropunctatus. J Comp Neurol. 1977; 176:539–557. [PubMed: 303647]

Bruce LL, Butler AB. Telencephalic connections in lizards. II. Projections to anterior dorsal ventricular ridge. J Comp Neurol. 1984; 229:602–615. [PubMed: 6209314]

Buckley K, Kelly RB. Identification of a transmembrane glycoprotein specific for secretory vesicles of neuronal and endocrine cells. J Cell Biol. 1985; 100:1284–1294. [PubMed: 2579958]

Burger, R.; Rubel, E. Encoding of interaural timing for binaural hearing. In: Kaas, J., editor. Evolution of nervous systems. Elsevier; New York: 2007.

Caicedo A, d'Aldin C, Puel JL, Eybalin M. Distribution of calcium-binding protein immunoreactivities in the guinea pig auditory brainstem. Anat Embryol. 1996; 194:465–487. [PubMed: 8905014]

Cant NB, Benson CG. Parallel auditory pathways: projection patterns of the different neuronal populations in the dorsal and ventral cochlear nuclei. Brain Res Bull. 2003; 60:457–474. [PubMed: 12787867]

Carr, CE. The evolution of the central auditory system in reptiles and birds. In: Webster, DB.; Fay, RR.; Popper, AN., editors. The evolutionary biology of hearing. Springer-Verlag; New York: 1992. p. 511-544.

Carr, CE.; Code, RA. The central auditory system of reptiles and birds. In: Dooling, RJ.; Fay, RR.; Popper, AN., editors. Comparative hearing: birds and reptiles. Springer; New York: 2000. p. 197-248.

Carr CE, Fujita I, Konishi M. Distribution of GABAergic neurons and terminals in the auditory system of the barn owl. J Comp Neurol. 1989; 286:190–207. [PubMed: 2794115]

Caspary DM, Havey DC, Faingold CL. Effects of micro-iontophoretically applied glycine and GABA on neuronal response patterns in the cochlear nuclei. Brain Res. 1979; 172:179–185. [PubMed: 466463]

Celio MR. Calbindin D-28K and parvalbumin in the rat nervous system. Neuroscience. 1990; 35:375–475. [PubMed: 2199841]

Celio MR, Heizmann CW. Calcium-binding protein parvalbumin as a neuronal marker. Nature. 1981; 293:300–301. [PubMed: 7278987]

Chiappe ME, Kozlov AS, Hudspeth AJ. The structural and functional differentiation of hair cells in a lizard's basilar papilla suggests an operational principle of amniote cochleas. J Neurosci. 2007; 27:11978–11985. [PubMed: 17978038]

Christensen-Dalsgaard J, Carr CE. Evolution of a sensory novelty: tympanic ears and the associated neural processing. Brain Res Bull. 2008; 75:365–370. [PubMed: 18331899]

Christensen-Dalsgaard J, Manley GA. Directionality of the lizard ear. J Exp Biol. 2005; 208:1209–1217. [PubMed: 15767319]

Christensen-Dalsgaard J, Manley GA. Acoustical coupling of lizard eardrums. J Assoc Res Otolaryngol. 2008; 9:407–416. [PubMed: 18648878]

Christensen-Dalsgaard, J.; Tang, YZ.; Carr, CE. Assoc Res Otolaryngol Abstr. 2007. Anatomy and physiology of binaural neurons in the brain stem of lizards; p. 544

Covey, E.; Carr, CE. The auditory midbrain in bats and birds. In: Schreiner, C.; Winer, JA., editors. The inferior colliculus. Springer; New York: 2005. p. 493-536.

Dávila JC, Guirado S, Puelles L. Expression of calcium-binding proteins in the diencephalon of the lizard *Psammodromus algirus*. J Comp Neurol. 2000; 427:67–92. [PubMed: 11042592]

Díaz C, Yanes C, Trujillo CM, Puelles L. Cytoarchitectonic subdivisions in the subtectal midbrain of the lizard Gallotia galloti. J Neurocytol. 2000; 29:569–593. [PubMed: 11283413]

Eatock R, Manley G, Pawson L. Auditory nerve fibre activity in the tokay gecko. J Comp Physiol A Neuroethol Sens Neural Behav Physiol. 1981; 142:203–218.

Ellis JH, Richards DE, Rogers JH. Calretinin and calbindin in the retina of the developing chick. Cell Tissue Res. 1991; 264:197–208. [PubMed: 1878940]

Erulkar S. Development of some mechanisms useful in sound localization. Fed Proc. 1974; 33:1928–1932. [PubMed: 4210562]

Foster RJ, Hall WJ. The organization of central auditory pathways in a reptile, Iguana iguana. J Comp Neurol. 1978; 178:783–832. [PubMed: 632382]

Fujita I, Konishi M. The role of GABAergic inhibition in processing of interaural time difference in the owl's auditory system. J Neurosci. 1991; 11:722–739. [PubMed: 2002359]

Grothe, B.; Carr, CE.; Casseday, JH.; Fritzsch, B.; Köppl, C. The evolution of central pathways and their neural processing patterns. In: Manley, GA.; Popper, AN.; Fay, RR., editors. Evolution of the vertebrate auditory system. Springer; New York: 2005. p. 289-359.

Hack NJ, Wride MC, Charters KM, Kater SB, Parks TN. Developmental changes in the subcellular localization of calretinin. J Neurosci. 2000; 20:RC67. [PubMed: 10729356]

Hartline PH, Campbell HW. Auditory and vibratory responses in the midbrains of snakes. Science. 1969; 163:1221–1223. [PubMed: 5765340]

Huesa G, Ikenaga T, Bottger B, Finger TE. Calcium-fluxing glutamate receptors associated with primary gustatory afferent terminals in goldfish (*Carassius auratus*). J Comp Neurol. 2008; 506:694–707. [PubMed: 18067143]

Ikenaga T, Huesa G, Finger TE. Co-occurrence of calcium-binding proteins and calcium-permeable glutamate receptors in the primary gustatory nucleus of goldfish. J Comp Neurol. 2006; 499:90–105. [PubMed: 16958099]

Kennedy MC. Auditory multiple-unit activity in the midbrain of the Tokay gecko (Gekko gekko, L.). Brain Behav Evol. 1974; 10:257–264. [PubMed: 4455355]

Kennedy MC, Browner RH. The torus semicircularis in a gekkonid lizard. J Morphol. 1981; 169:259–274.

Köppl C, Authier S. Quantitative anatomical basis for a model of micromechanical frequency tuning in the Tokay gecko, Gekko gecko. Hear Res. 1995; 82:14–25. [PubMed: 7744709]

Kubke MF, Carr CE. Morphological variation in the nucleus laminaris of birds. Int J Comp Psychol. 2006; 19:83–97.

Kubke MF, Gauger B, Basu L, Wagner H, Carr CE. Development of calretinin immunoreactivity in the brainstem auditory nuclei of the barn owl (Tyto alba). J Comp Neurol. 1999; 415:189–203. [PubMed: 10545159]

Kunzle H. Projections from the cochlear nuclear complex to rhombencephalic auditory centers and torus semicircularis in the turtle. Brain Res. 1986; 379:307–319. [PubMed: 3742224]

Lachica EA, Rubsamen R, Rubel EW. GABAergic terminals in nucleus magnocellularis and laminaris orginate from the superior olivary nucleus. J Comp Neurol. 1994; 348:403–418. [PubMed: 7844255]

Lohmann C, Friauf E. Distribution of the calcium-binding proteins parvalbumin and calretinin in the auditory brainstem of adult and developing rats. J Comp Neurol. 1996; 367:90–109. [PubMed: 8867285]

Manley, GA. A review of the auditory physiology of reptiles. In: Autrum, H.; Perl, E.; Schmidt, RF., editors. Progress in sensory physiology. Springer Verlag; Berlin: 1981. p. 49-134.

Manley, GA. Peripheral hearing mechanisms in reptiles and birds. Springer-Verlag; New York: 1990.

Manley GA. Evolution of structure and function of the hearing organ of lizards. J Neurobiol. 2002; 53:202–211. [PubMed: 12382276]

Manley GA, Köppl C, Sneary M. Reversed tonotopic map of the basilar papilla in *Gekko gecko*. Hear Res. 1999; 131:107–116. [PubMed: 10355608]

Marcellini, DL. The acoustic behavior of lizards. In: Greenberg, N.; MacLean, PD., editors. Behavior and neurology of lizards. U.S. Department of Health, Education and Welfare; Rockville, MD: 1977. p. 287-300.

Marin F, Puelles L. Morphological fate of rhomboneres in quail/chick chimeras: a segmental analysis of hindbrain nuclei. Eur J Neurosci. 1995; 7:1714–1738. [PubMed: 7582126]

Miller MR. The cochlear nuclei of lizards. J Comp Neurol. 1975; 159:375–406. [PubMed: 1112916]

Miller MR. The cochlear nuclei of snakes. J Comp Neurol. 1980; 192:717–736. [PubMed: 7419751]

Miller MR, Kasahara M. The cochlear nuclei of some turtles. J Comp Neurol. 1979; 185:221–236. [PubMed: 429618]

Morona R, González A. Immunohistochemical localization of calbindin-D28k and calretinin in the brainstem of anuran and urodele amphibians. J Comp Neurol. 2009; 515:503–537. [PubMed: 19479990]

Müller CM. c-Aminobutyric acid immunoreactivity in brainstem auditory nuclei of the chicken. Neurosci Lett. 1987; 77:272–276. [PubMed: 3302766]

Nealen PM. An interspecific comparison using immunofluorescence reveals that synapse density in the avian song system is related to sex but not to male song repertoire size. Brain Res. 2005; 1032:50–62. [PubMed: 15680941]

Otis TS, Raman IM, Trussell LO. AMPA receptors with high Ca^{2+} permeability mediate synaptic transmission in the avian auditory pathway. J Physiol. 1995; 482:309–315. [PubMed: 7714824]

Parks TN, Code RA, Taylor DA, Solum DA, Strauss KI, Jacobowitz DM, Winsky L. Calretinin expression in the chick brainstem auditory nuclei develops and is maintained independently of cochlear nerve input. J Comp Neurol. 1997; 383:112–121. [PubMed: 9184990]

Pollak GD, Burger RM, Park TJ, Klug A, Bauer EE. Roles of inhibition for transforming binaural properties in the brainstem auditory system. Hear Res. 2002; 168:60–78. [PubMed: 12117510]

Pór A, Pocsai K, Rusznák Z, Szucs G. Presence and distribution of three calcium binding proteins in projection neurons of the adult rat cochlear nucleus. Brain Res. 2005; 1039:63–74. [PubMed: 15781047]

Pritz MB. Ascending connections of a midbrain auditory area in a crocodile, Caiman crocodilus. J Comp Neurol. 1974; 153:179–198. [PubMed: 4359288]

Puelles L, Robles C, Martinez-de-la-Torre M. New subdivision schema for the avian torus semicircularis: Neuro-chemical maps in the chick. J Comp Neurol. 1994; 340:98–125. [PubMed: 8176005]

Raman IM, Trussell LO. Concentration-jump analysis of voltage-dependent conductances activated by glutamate and kainate in neurons of the avian cochlear nucleus. Biophys J. 1995; 69:1868–1879. [PubMed: 8580330]

Robles-Moreno, C. Estudio comparado de la subdivision quimioarquitectonica del complejo toral del mesencefalo en el pollo y en la Tarentola mauretanica. University de Murcia; Doctorado en Medicina (MD): 1995. p. 157Puelles L, Martínez de la Torre Fox M, directores

Rogers JH. Calretinin: a gene for a novel calcium-binding protein expressed principally in neurons. J Cell Biol. 1987; 105:1343–1353. [PubMed: 3654755]

Rouiller, E. Functional organization of auditory pathways. In: Ehret, G.; Roman, R., editors. The central auditory system. Oxford University Press; Oxford: 1997. p. 3-96.

Schneggenburger R, Neher E. Presynaptic calcium and control of vesicle fusion. Curr Opin Neurobiol. 2005; 15:266–274. [PubMed: 15919191]

Schreiner, C.; Winer, JA. The inferior colliculus. Springer; New York: 2005.

Sloviter RS, Nilaver G. Immunocytochemical localization of GABA-, cholecystokinin-, vasoactive intestinal polypeptide-, and somatostatin-like immuoreactivity in the area dentata and hippocampus of the rat. J Comp Neurol. 1987; 256:42–60. [PubMed: 3819038]

Smeets W, López J, González A. Distribution of neuro-peptide FF-like immunoreactivity in the brain of the lizard Gekko gecko and its relation to catecholaminergic structures. J Comp Neurol. 2006; 498:31–45. [PubMed: 16856160]

Szpir MR, Sento S, Ryugo DK. The central projections of the cochlear nerve fibers in the alligator lizard. J Comp Neurol. 1990; 295:530–547. [PubMed: 2358519]

Szpir MR, Wright DD, Ryugo DK. Neuronal organization of the cochlear nuclei in alligator lizards: a light and electron microscopic investigation. J Comp Neurol. 1995; 357:217–241. [PubMed: 7665726]

Takahashi TT, Keller CH. Commissural connections mediate inhibition for the computation of interaural level difference in the barn owl. J Comp Physiol A. 1992; 170:161–169. [PubMed: 1374800]

Takahashi TT, Konishi M. Projections of nucleus angularis and nucleus laminaris to the lateral lemniscal nuclear complex of the barn owl. J Comp Neurol. 1988a; 274:212–238. [PubMed: 2463287]

Takahashi TT, Konishi M. Projections of the cochlear nuclei and nucleus laminaris to the inferior colliculus of the barn owl. J Comp Neurol. 1988b; 274:190–211. [PubMed: 2463286]

Takahashi TT, Carr CE, Brecha N, Konishi M. Calcium binding protein-like immunoreactivity labels the terminal field of nucleus laminaris of the barn owl. J Neurosci. 1987; 7:1843–1856. [PubMed: 2439666]

Takahashi TT, Barberini CL, Keller CH. An anatomical substrate for the inhibitory gradient in the VLVp of the owl. J Comp Neurol. 1995; 358:294–304. [PubMed: 7560288]

Tang Y-Z, Zhuang L, Wang Z, McEachran J. Advertisement calls and their relation to reproductive cycles in Gekko gecko (Reptilia, Lacertilia). Copeia. 2001; 2001:248–253.

ten Donkelaar, H. Reptiles, the central nervous system of vertebrates. Vol. vol 2. Springer; Berlin: 1998.

ten Donkelaar HJ, Bangma GC, Barbas-Henry HA, de Boer-van Huizen R, Wolters JG. The brain stem in a lizard, *Varanus exanthematicus*. J Comp Neurol. 1987; 103:56–60.

Trussell LO. Synaptic mechanisms for coding timing in auditory neurons. Annu Rev Physiol. 1999; 61:477–496. [PubMed: 10099698]

Trussell, LO. Central synapses that preserve auditory timing. In: Oertel, D., editor. The senses: a comprehensive reference. Elsevier; New York: 2008. p. 587-602.

Vidal N, Hedges SB. The molecular evolutionary tree of lizards, snakes, and amphisbaenians. C R Biol. 2009; 332:129–139. [PubMed: 19281946]

von Bartheld C, Code RA, Rubel EW. GABAergic neurons in brainstem auditory nuclei of the chick: distribution, morphology, and connectivity. J Comp Neurol. 1989; 287:470–483. [PubMed: 2477407]

Wagner H, Mazer JA, von Campenhausen M. Response properties of neurons in the core of the central nucleus of the inferior colliculus of the barn owl. Eur J Neurosc. 2002; 15:1343–1352.

Wever, EG. The reptile ear. Princeton University Press; Princeton, NJ: 1978.

Wild JM. Nuclei of the lateral lemniscus project directly to the thalamic auditory nuclei in the pigeon. Brain Res. 1987; 408:303–307. [PubMed: 2439168]

Wild JM, Kubke MF, Carr CE. Tonotopic and somatotopic representation in the nucleus basalis of the barn owl, Tyto alba. Brain Behav Evol. 2001; 57:39–62. [PubMed: 11359047]

Wild J, Kubke M, Pena J. A pathway for predation in the brain of the barn owl (Tyto alba): projections of the gracile nucleus to the “claw area” of the rostral wulst via the dorsal thalamus. J Comp Neurol. 2008; 509:156–166. [PubMed: 18461603]

Wild J, Kruetzfeldt N, Kubke M. Afferents to the cochlear nuclei and nucleus laminaris from the ventral nucleus of the lateral lemniscus in the zebra finch (Taeniopygia guttata). Hear Res. 2009; 257:1–7. [PubMed: 19631727]

Zeng S-J, Xi C, Zhang X-W, Zuo M-X. Differences in neurogenesis differentiate between core and shell regions of auditory nuclei in the turtle (Pelodiscus sinensis): evolutionary implications. Brain Behav Evol. 2007; 70:174–186. [PubMed: 17595537]

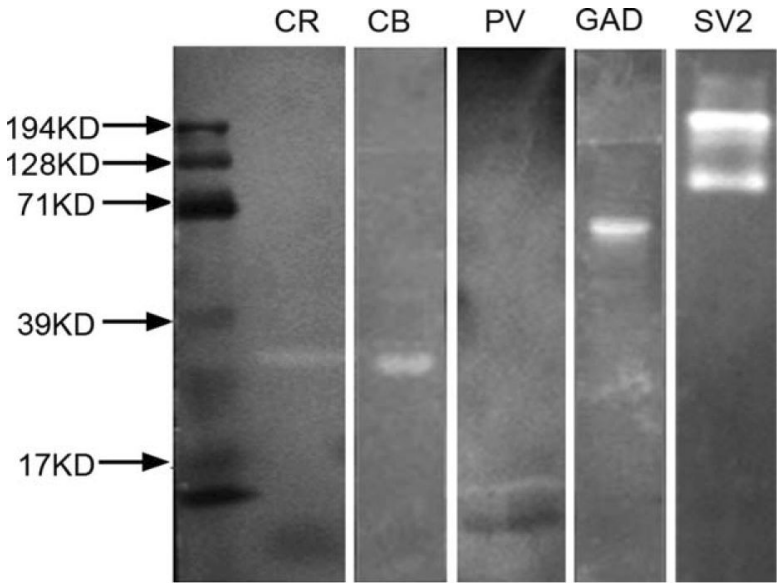

Figure 1.
Western blots for CBPs, GAD, and SV2 in gecko brain. All blots except that for SV2 yield a single band at estimated molecular weights of 29 kD, 28 kD, 65–67 kD, 15 kD, and about 200 kD for CR, CB, GAD, PV, and SV2 respectively.

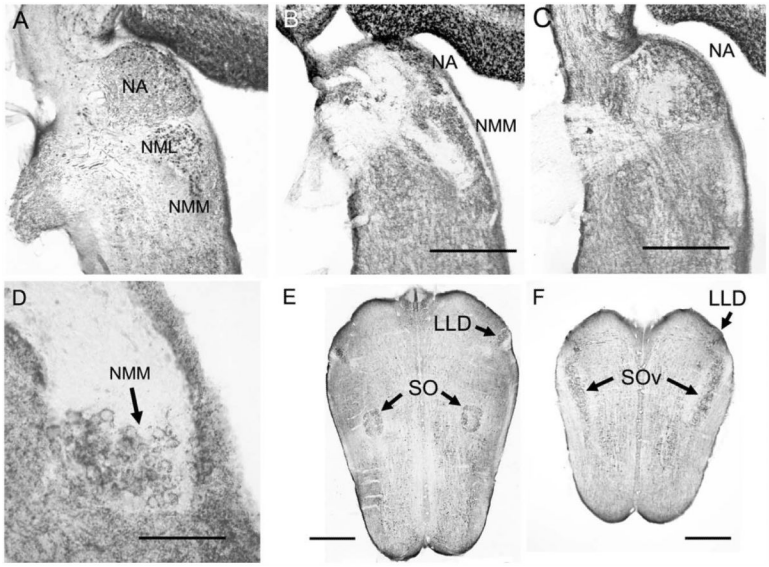

Figure 2.

Calcium-binding protein and SV2 immunoreactivity in horizontal sections. **A:** NM, NML, and NA are CR-ir and innervated by CR-ir auditory nerve fibers. **B,C:** SV2 immunoreactivity is absent in the auditory nerve and thus reveals the unlabeled dorsal-caudal fiber bundle (B) bifurcating to the dorsal NMM, lateral NML, and lateral NA. The ventral-rostral fiber bundle (C) projects to medial NA. **D:** SV2 immunoreactivity in NMM reveals SV2-ir perisomatic terminals. **E:** CR immunoreactivity in LLD and SO. **F:** In a more ventral section, CR-ir terminals in lemniscal nuclei and SOv. CR-ir fibers connect the olivary and lemniscal nuclei. Scale bar = 400 μm B (applies to A,B); 400 μm C; 100 μm in D; 600 μm in E,F.

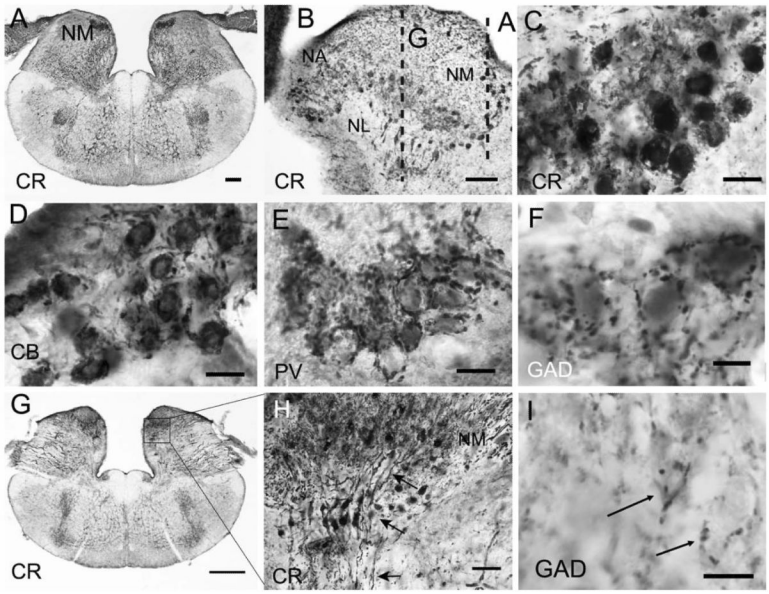

Figure 3.

Calcium-binding protein and GAD immunoreactivity in nucleus magnocellularis and nucleus laminaris. **A,C**: CR heavily labeled both cell bodies and axonal arbors of NM neurons in transverse sections. **B**: Sagittal section reveals CR-ir neurons and fibers in NM, NA, and NL; dashed lines indicate the plane of section for A,G. **D**: PV-ir auditory nerve terminals surround NM neurons. **E**: CB-ir labels auditory nerve fibers and terminals and also lightly labels NM neurons. **F**: GAD-ir terminals surround unlabeled somata in NM. **G**: More rostral section shows NM, NL, and the SO and SOv. **H**: Enlarged region showing two strands of CR-ir NL bipolar cells ventral to NM; arrows point to dorsal dendrites, cell body, and ventral dendrites. **I**: GAD-ir terminals surround unlabeled somata in NL. Scale bars = 200 μm in A; 100 μm in B; 20 μm in C–E; 10 μm in F,I; 500 μm in G; 50 μm in H.

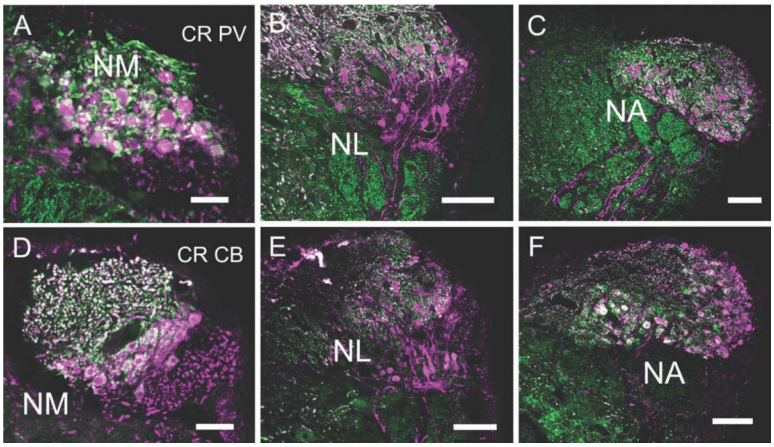

Figure 4.

Fluorescence double labeling of calcium-binding proteins in NM, NL, and NA. The top row shows CR (cyan) and PV (green) immunoreactivity, while the bottom row shows CR and CB (green), all in transverse sections, with medial to the right. **A,D**: NM. A: CR- and PV-ir labels many axons and terminals around CR-ir NM neurons. Note double labeled (white) auditory nerve terminals. D: CB and CR are co-localized in the auditory nerve terminals and in NM cytoplasm, with CB found in a ring under the cell membrane. **B,E**: NL. B: PV was absent from NL, although double labeled PV and CR labeled the auditory nerve fibers above NL in NM. CR-ir in NL shows a similar staining pattern as in the HRP immunohistochemistry (Figure 3H). E: CB-ir was present at low levels in NM cytoplasm, but not detected in NL. CR-ir fibers descended to eventually coalesce into the lemniscus, below SO. **C,F**: NA. C: NA cell bodies are CR-ir, while PV is only localized to terminals around neurons. F: CR heavily labeled many cell bodies in the medial area of NA. Some more lateral neurons expressed both CR and CB, and some neurons express either CR or GB. Note CR-ir fibers descended to join lemniscal fibers. Scale bars = 100 μm.

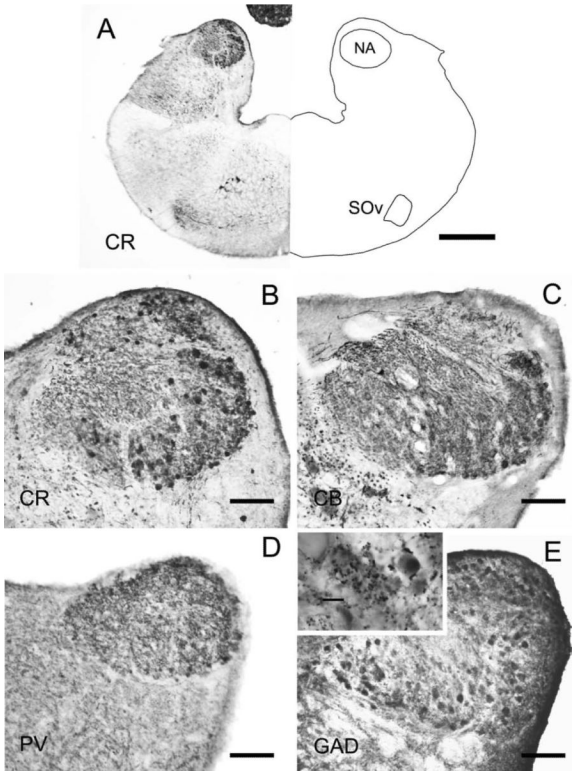

Figure 5.

Calcium-binding protein immunoreactivity in nucleus angularis. **A**: Transverse hemisection at the level of NA paired with a line drawing. **B–E**: Neurons in medial NA are intensely CR-ir, although few neurons are CB- or PV-ir; CB and PV only labeled presumed auditory nerve terminals in NA. Some neurons are GAD-ir, and GAD-ir terminals are distributed throughout the neuropil. Scale bars = 500 μm in A; 100 μm in B–E; 10 μm in inset.

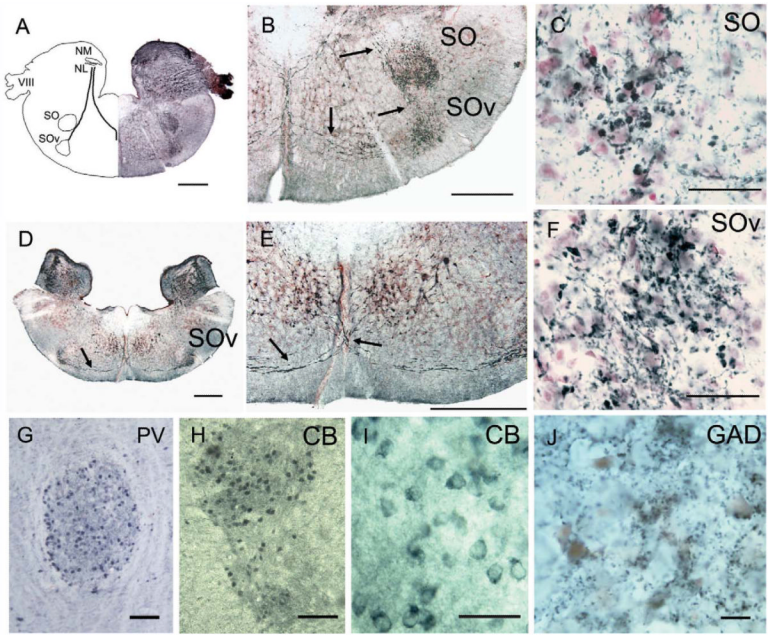

Figure 6.

Calretinin terminals in the superior olivary nuclei. **A**: Transverse section through the medulla at the level of NM and SO, paired with a drawing to show the CR-ir tract connecting the first-order nuclei with the SO and SOv (black lines). CR-ir fibers delineate the projection to the ipsilateral SO and SOv, and to the contralateral SOv. **B**: Higher magnification view of CR-ir in SO and SOv. Arrows show the CR-ir fiber tracts to SO, between SO and SOv, and the midline decussation between first-order nuclei and contralateral SOv. **C**: Large CR-ir terminals in the SO. **D**: More rostral transverse section through the medulla at the level of NA and SOv shows CR-ir fibers that decussate and connect first-order nuclei and SOv (arrow). **E**: Enlarged view of the decussating CR-ir tract (arrows). **F**: Large CR-ir terminals in both the SO and the SOv; note large perisomatic boutons in SOv. **G**: Neurons in both SO and SOv are PV-ir, SO shown in horizontal section. **H,I**: CB-ir labeled neurons in SO. **J**: GAD-ir terminals in SO, both perisomatic and distributed through the neuropil. Scale bars = 500 at μm in A,B,D,E; 50 μm in C,F; 100 μm in G,H; 20 μm inl; 10 μm in J. [Color figure can be viewed in the online issue, which is available at www.interscience.wiley.com.]

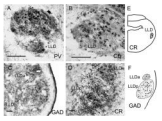

Figure 7.

Calcium-binding protein and GAD immunoreactivity in LLD. **A,B**: Horizontal sections through LLDp, with lateral to the right, rostral to the top. A: PV-ir neurons and neuropil in LLD. B: CB-ir neurons. **C,D**: Tranverse sections through LLD, with lateral right. C: GAD-ir cells and terminals in LLDp and LLDa. D: CR-ir terminals surround unlabeled cell bodies in both LLDa and LLDp. **E**: Schematic transverse section at the level of the lemniscal nuclei, with stippling indicating CR-ir terminals. **F**: Schematic cross-section through lemniscal nuclei showing the distribution of GAD-ir cells and terminals. Scale bars = 100 μm.

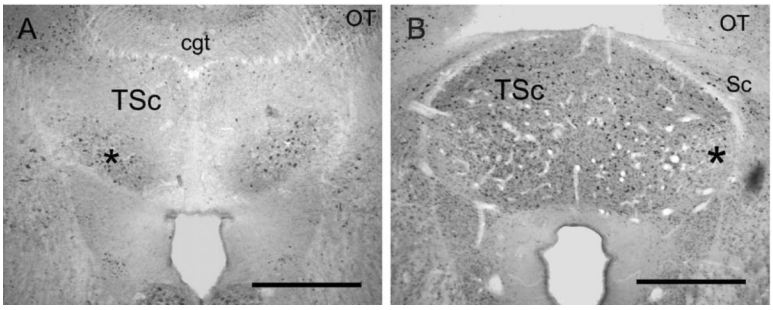

Figure 8.

Calbindin and parvalbumin immunoreactivity in TSc. **A**: PV-ir cell bodies and neuropil predominate in the ventral TSc (asterisk). **B**: CB-ir delineates the TSc. Note the decreased C**B**-ir expression in the lateral region of TSc that receives CR-ir terminals (asterisk). cgt, Commissure of griseum tectale; OT, optic tectum; Sc, preisthmic superficial area. Scale bars = 500 μm.

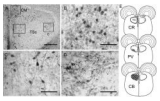

Figure 9.

Calretinin-ir neurons and terminals in the torus semicircularis. **A**: Transverse section through the caudal torus. CR-ir neurons are abundant in the caudomedial shell nucleus (CM), formerly called the laminar nucleus (B) and marked the boundary of central nucleus of the torus (TSc; also termed toral nucleus or To by Puelles et al., 1994). **B**: CR-ir in CM. **C**: CR-ir neurons with long dendrites at medial-dorsal border between CM and TSc. **D**: CR-ir terminals in the lateral TSc. **E**: Schematic cross-sections. Scale bars = 200 μm in A; = 50 μm in B–D.

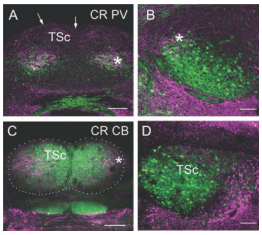

Figure 10.

Fluorescence double labeling of calcium-binding proteins in the torus semicircularis. Transverse sections through caudal (**A,C**), middle (**B**), and rostral (**D**) levels of TSc. Medial is to the right for both B and D. A,B: CR (cyan) and PV: A: In caudal torus, CR labeled terminals in the lateral portion of TSc (compare with CR-ir terminals in Figure 10D). At this very caudal level, most PV-ir neurons overlapped with the CR-ir terminals (asterisk). Arrows mark the pial surface. B: In TSc (left), the ventral PV-ir neuron region extends laterally from the CR-ir terminal recipient region (asterisk) to the ventromedial Tsc (compare with the PV-ir label here and in Fig. 11). Some CR-ir terminals surrounded PV-ir neurons. C: CR and CB in caudal torus (outlined by dots). CR-ir terminals (asterisk) were confined to lateral TSc, whereas CB-ir defined the entire TSc. D: CR and CB in rostral torus. There are few CR-ir terminals in the TSc, but CB-ir defines the extent of TSc. Scale bars = 100 μm in A,C; 200 μm in B,D.

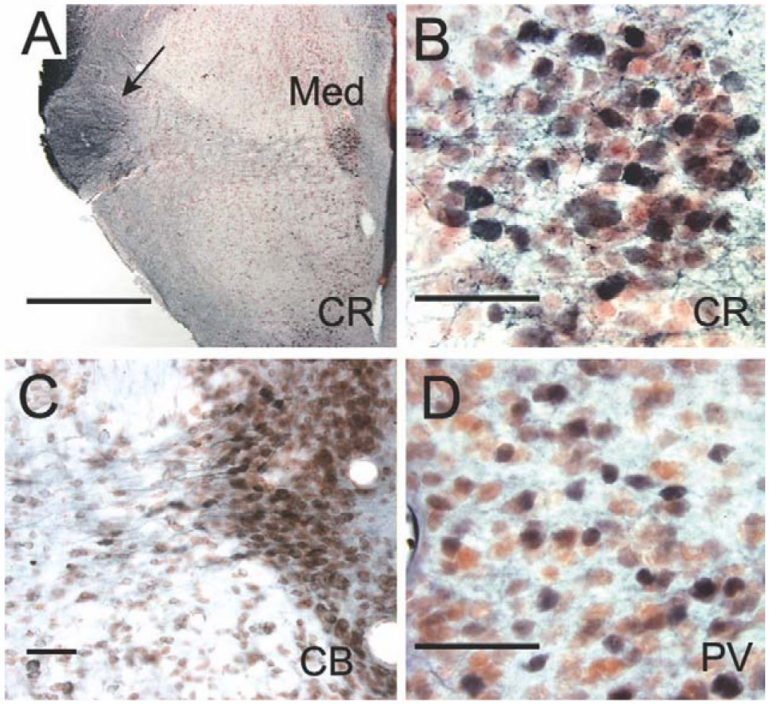

Figure 11.

Calcium-binding proteins in the nucleus medialis of the thalamus. **A,B**: CR-ir. **C**: CB-ir. **D**: PV-ir. Many cell bodies in nucleus medialis (Med) are CR-ir and CB-ir, and some are PV-ir. CR-ir fibers project laterally (arrow). Scale bars = 500 μm in A; 50 μm in B–D. [Color figure can be viewed in the online issue, which is available at www.interscience.wiley.com.]

TABLE 1

Antibody Characterization

Antibody	Immunogen	Manufacturer and type
Calretinin	Recombinant human calretinin	Swant 7699/66, rabbit polyclonal
Parvalbumin	parvalbumin from carp muscle	Swant PA-235, mouse monoclonal
Calbindin	Chicken gut calbindin D28k	Swant 300, mouse monoclonal
Glutamic acid decarboxylase 65/67	C-terminal region of human GAD67 (amino acids 579–594).	Sigma G5163, rabbit polyclonal
Synaptic vesicle protein 2	Synaptic vesicles from *Ommata* electric organ	SV2, Hybridoma Bank, University of lowa, mouse monoclonal

TABLE 2

Distribution of Calcium-Binding Protein- and Glutamic Acid Decarboxylase-lmmunoreactive Cells in *Gekko gecko*

Antibody	Calretinin	Parvalbumin	Calbindin	Glutamic acid decarboxylase
Vlllth nerve	+++	+++	+++	
Nucleus magnocellularis	+++		+	
Nucleus angularis	+++	+	+	+
Nucleus laminaris	+++			
Superior olive		+++	+++	+
Ventral superior olive		+++	++	+
Dorsal nucleus of lateral lemniscus		++	++	+++
Torus semicircularis, central nucleus	++	++	+++	++
Nucleus medialis of the thalamus	++	+	++	